APPENDICES

APPENDIX 1
WIND ENVIRONMENT AT THE SITE

A detailed analysis of historical winds was not made for this study, but the results of a previous study, made specifically for the Golden Gate Bridge, Highway and Transportation District were used (Ref 5).

For a bridge that is a vital transportation link in a major disaster, it is appropriate that the design wind speed be a wind speed with a return period of at least 100 years. An omnidirectional, one hour averaged wind speed, at the bridge deck elevation, with a return period of 100 years, was found to be 76 mph (Ref 5).

An aeroelastic flutter instability can be catastrophic (as it was for the Tacoma Narrows Bridge). Consequently, it is appropriate to specify that an aeroelastic flutter instability should not occur for a wind speed with a return period less than 10,000 to 100,000 years. From the referenced historical wind speed analysis (Ref 5), such an appropriate critical flutter wind speed criterion was determined to be 100 mph. This is a 10-minute averaged wind speed at the bridge deck elevation (70.87 m).

Strong winds are most likely to come from the south and the west. See Figure 1.1, taken from Ref 5. Also note that, at the site, the percentage of time that strong winds (with a return period of 100 years or more) come from the east is three orders of magnitude lower than the percentage of time that strong winds come from the west. Probabilities are proportional to the percentages, and return periods are proportional to the inverse of the probabilities. Therefore, the return period for equal wind speeds from the east will have a return period approximately 1,000 times longer than the return period for a comparable wind speed from the west. Winds from the west are critical.

An omnidirectional 100 year wind (essentially equal to a 100 year wind from the south or the west) of 34 m/s (76 mph) was determined. It is reasonable to assume, therefore, from Figure 1.1 in Ref 5 that this wind speed, 34 m/s (76 mph, would have a return period of 100,000 years for winds from the east. Assuming that the distribution of annual extremes at the site, for winds from the east, are similar to those from the west, it can be computed that for winds from the east, an hour averaged wind speed of 20.6 m/s (46 mph) would have a return period of 100 years, and a 10-minute averaged wind speed of 29.5 m/s (66 mph) would have return period of 10,000 years. These are approximate values, but are suitable for the analyses for these non-critical directions.

Note that winds from the south may also be likely. However, winds that are essentially perpendicular to the axis of the bridge (the axis of the bridge is north-south) are critical from a stability and buffeting point of view.

FIGURE 1.1

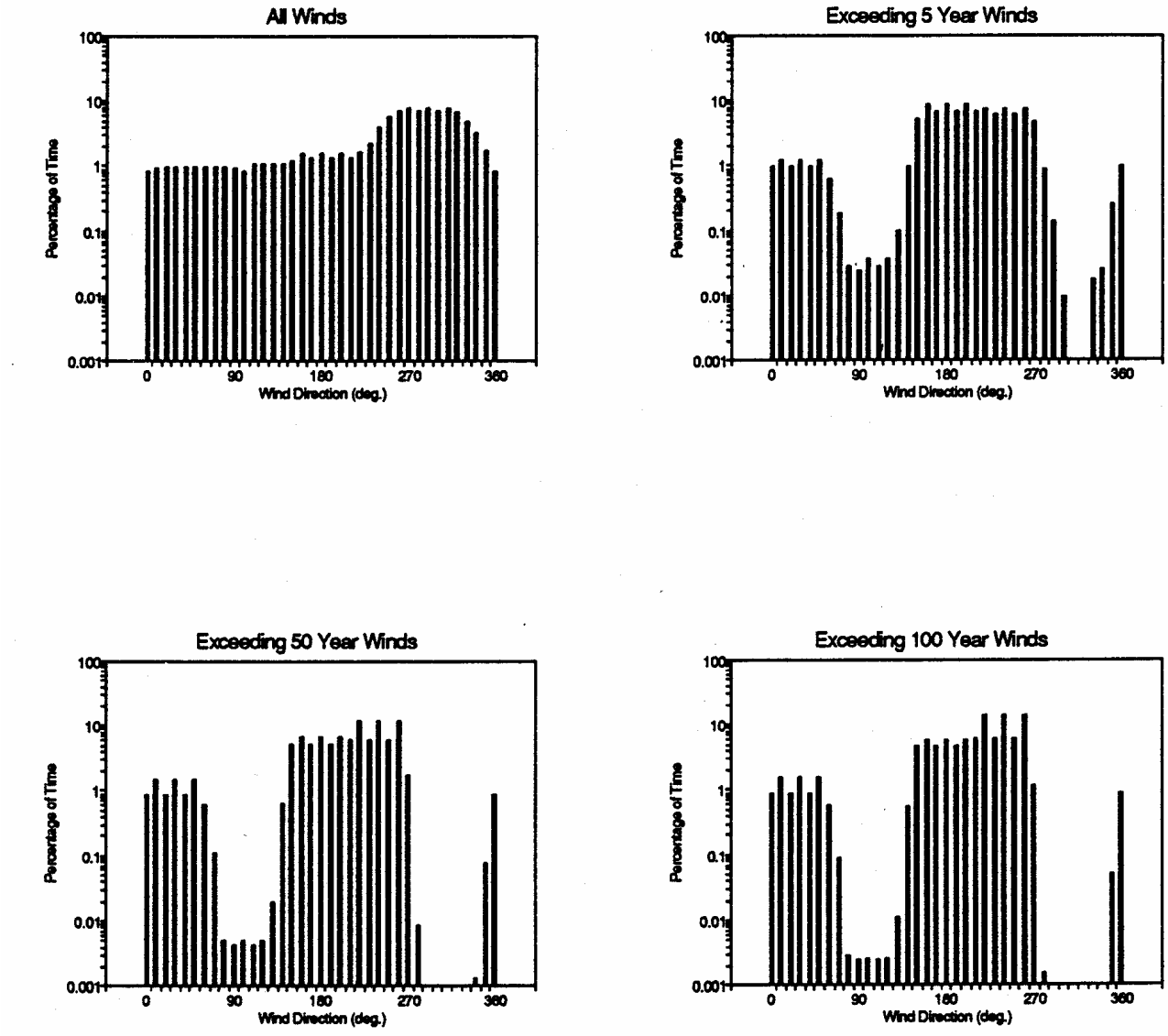
All Winds
Exceeding 5 Year Winds
Exceeding 50 Year Winds
Exceeding 100 Year Winds
Percentage of Time
100
10
1
0.1
0.01
0.001
0
90
180
270
360
Wind Direction (deg.)

APPENDIX 2
TEST FACILITIES

Wind tunnel tests were performed in the 1 x 4 m open return type atmospheric boundary layer wind tunnel, designed specifically for bridge section model and full-bridge model testing, owned and operated by the West Wind Laboratory, Inc. Drawings of the wind tunnel are shown on Figure 2.1. Wind speed profiles upstream and downstream from the section model test section are shown in Figures 2.2 and 2.3. Shown in Figure 2.4 is the boundary layer at one end plate. Wind speeds are continuously variable from 0 to 6.1 m/s.

The test section is open without walls or a ceiling. Ambient pressures within the test chamber therefore are essentially constant. Furthermore, winds can flow around and over the models without constriction (as in the full-scale environment). Therefore, blockage effects are minimal, i.e., wind speed will not be artificially accelerated around the model because there are no walls to constrict and accelerate the flow.

The wind tunnel extends 6.1 m upstream from the test section without flair or constriction. Atmospheric boundary layers can be generated in this space with the use of spires and blocks on the wind tunnel floor.

Model displacements, and force transducer displacements are measured with Macro Sensors PRH-812-050 LVDT Transducers and Macro Sensors LPC-2000 Signal Conditioners. Mean wind speeds are measured with a Sierra Instruments Model 618 Air Velocity Meter. Mean and fluctuating wind speeds are measured with a total head tube and Setra System, Inc. 239 Pressure Transducer.

Analog signals from the transducers are digitized on a ComputerBoards PCM-DAS08 Analog to Digital Converter.

FIGURE 2.1
1 X 4 m ATMOSPHERIC BOUNDARY LAYER WIND TUNNEL

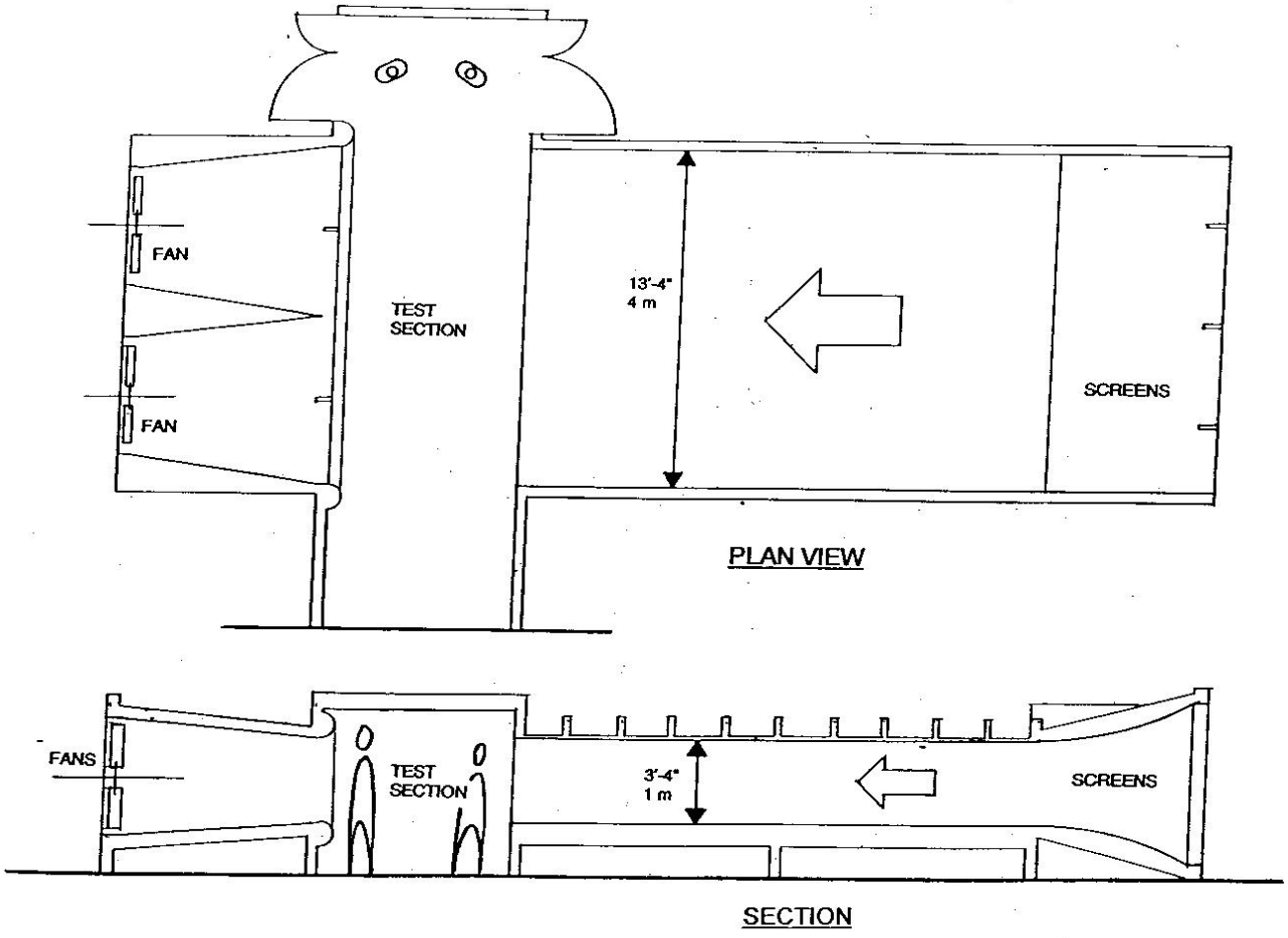

FIGURE 2.2

MEAN VELOCITY PROFILE
0.5 METER UPSTREAM

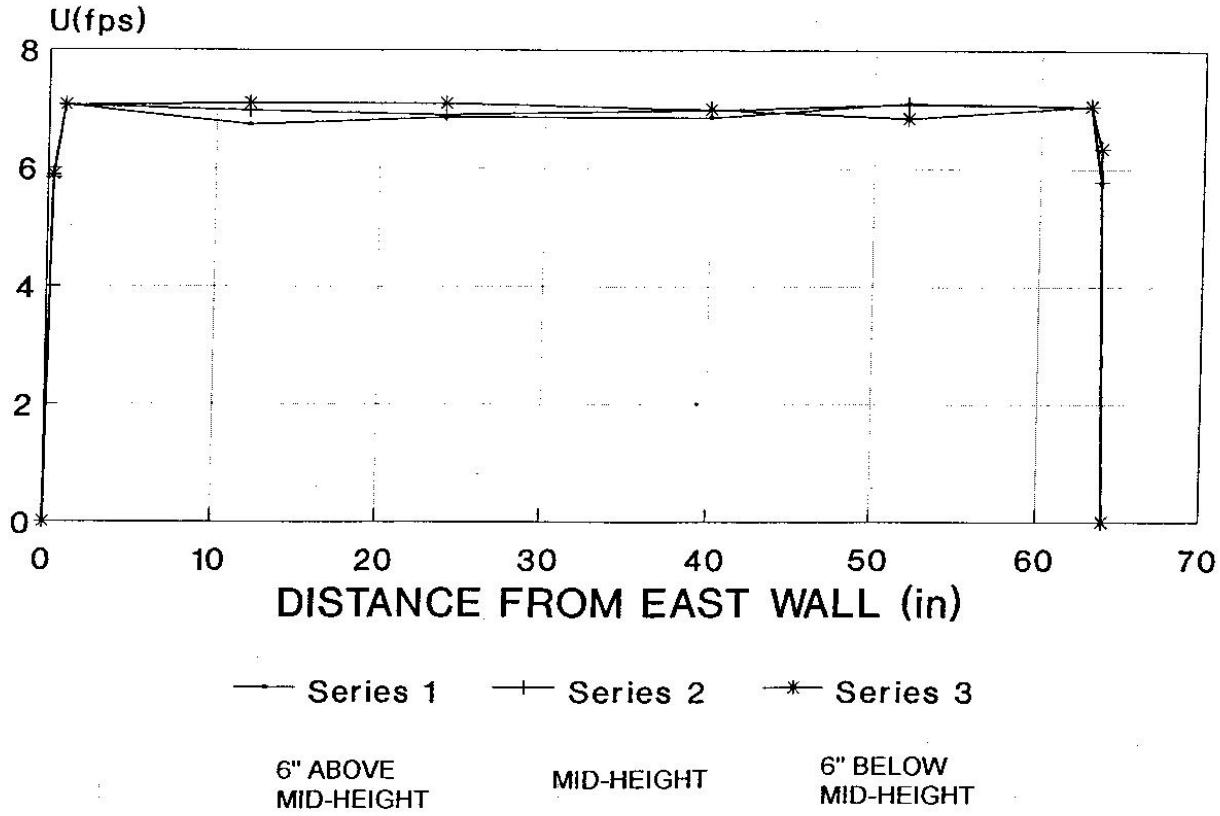

FIGURE 2.3

MEAN VELOCITY PROFILE
0.5 METER DOWNSTREAM

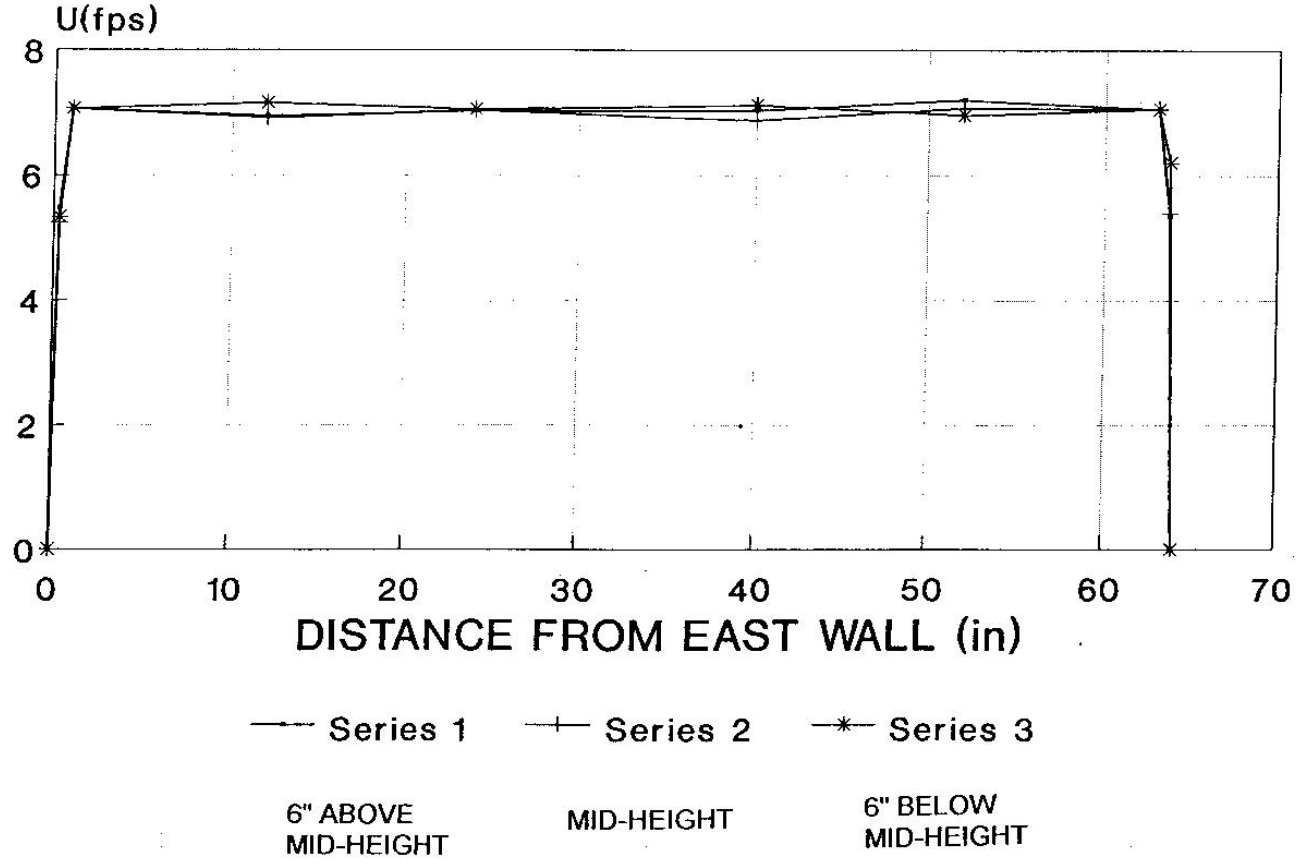

FIGURE 2.4

MEAN VELOCITY PROFILE
SIDE BOUNDARY LAYER

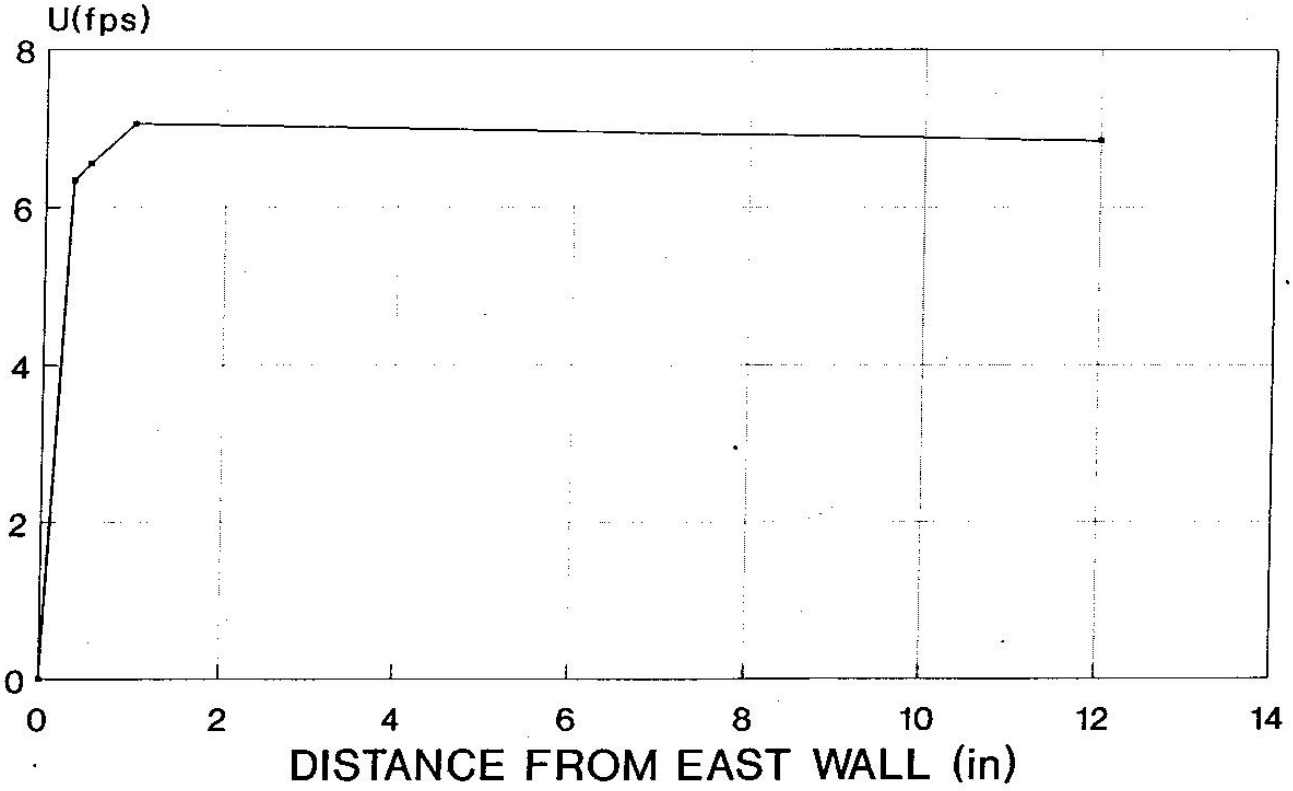

MID-HEIGHT

APPENDIX 3
PROCEDURE TO PREDICT FULL BRIDGE MOTIONS IN STRONG TURBULENT WINDS

The procedure described here differs from that presented in Ref 4 only in the description of the aerodynamic loads on the bridge deck. Otherwise, they are the same. Specifically, the bridge deck is divided into finite sized elements. On each, the aerodynamic load is computed including motion dependent terms and buffeting terms. Generalized actions are computed for each mode. The response of each mode is computed for the next time step using these generalized actions, the total physical bridge motions are then computed, new aerodynamic loads are computed on each element using these elemental physical motions, and the process is once again repeated for the next step in time. The three dimensional flow field was generated analytically as described in Ref 3.

Chen, Matsumoto, and Kareem describe in Ref 4 the motion dependent aerodynamic loads, in the time domain, for arbitrary motions, in terms of impulse functions. While not as elegant mathematically, the motion dependent aerodynamic loads can also be described directly in terms of the aeroelastic flutter derivatives. This description is computationally more efficient and it eliminates numerical uncertainties associated with one additional series of transformations (to obtain impulse functions from flutter derivatives).

Central to this description is the assumption that the motion dependent aerodynamic loads can be described as the superposition of modal, motion dependent, aerodynamic loads. This has been demonstrated to be valid for years. See Appendix 4.

Motion dependent aerodynamic lift, L_{ij} , and moment, M_{ij} , on the ith deck element, due to the jth mode of vibration can be given by Simiu and Scanlan (Ref 1)

$$L_{ij} = 1/2\rho U^2 B(KH_{1ij}^*((dhij / dt) / U) + KH_{2ij}^*(B(d\alpha ij / dt) / U) + K^2H_{3ij}^*\alpha_{ij} + K^2H_{4ij}^*(h_{ij}/B)) \qquad (3.1)$$

$$M_{ij} = 1/2\rho U^2 B^2(KA_{1ij}^*(dhij / dt) / U) + KA_{2ij}^*(B(d\alpha ij / dt) / U) + K^2A_{ij}^*\alpha_{ij} + K^2A_{4ij}^*(h_{ij}/B)) \qquad (3.2)$$

where ρ = air density, $K = \omega B/U$ and $\omega = 2\pi n$, and A_{1ij}^*, A_{2ij}^*, A_{3ij}^*, A_{4ij}^*, H_{1ij}^*, H_{2ij}^*, H_{3ij}^*, and H_{4ij}^* aeroelastic flutter derivatives. See Figure 3.1 for positive coordinate directions, and positive action directions. The aeroelastic flutter derivatives can be interpreted as frequency dependent aerodynamic stiffness and damping terms, valid for steady, decaying, or diverging harmonic motions. The flutter derivatives typically are obtained as those damping and stiffness terms that must have existed to produce the observed, superimposed torsional and vertical motions of a section model, each with its own frequency of vibration.

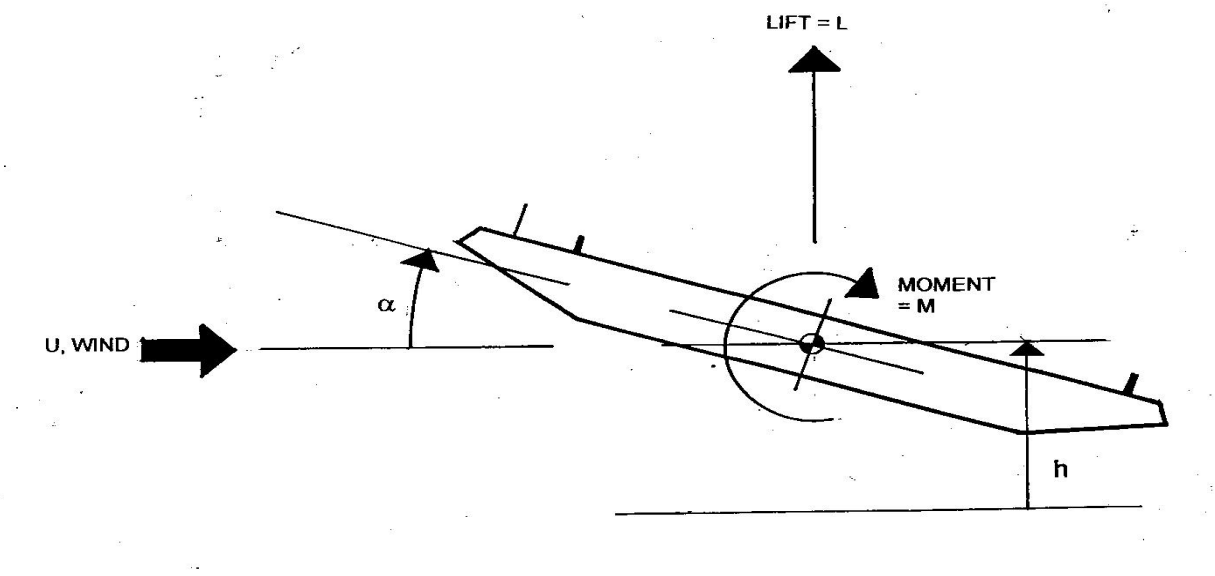

At the onset of each simulation, in smooth or turbulent flow, each mode is given a unit modal displacement. They are all released simultaneously. Although the bridge motion may look arbitrary and erratic, each mode of vibration typically is a slowly varying harmonic motion at a single frequency for which the flutter derivatives are valid. At the onset, each mode of vibration typically will vibrate near its aerodynamically stiffened (or softened) natural frequency. As the motion progresses, various modes will couple aerodynamically and gradually change their frequency to some other, but single, frequency of vibration.

The use of impulse functions, in convolution integrals, to describe the motion dependent aerodynamic loads on a bridge deck, is essentially equivalent to the use of continuously variable (with respect to frequency) flutter derivatives in (3.1) and (3.2). Because the products of K or K^2 and the flutter derivatives vary so slowly with frequency, the flutter derivatives can be varied at finite steps in time (as required), instead of being varied continuously, without loss of precision (certainly with respect to the experimental errors associated with the experimentally obtained flutter derivatives and associated impulse functions). In this procedure, at 20 second intervals (in a 10-minute simulation) all products of K or K^2 and the corresponding flutter derivatives are re-evaluated, for each element, for each mode of vibration, based upon the average frequency of vibration for the preceding 20-second time segment, for the mode in question and based upon the average wind speed for that 20-second time segment. The average 20-second wind speeds, and fluctuating wind speeds about that average, are used to compute the aerodynamic loads.

In this simulation procedure, a simplified, quasi-steady form of the buffeting forces (Ref 1) is also used. This is a conservative assumption, but it is not assumed to be too conservative. For normal values of U/nB at design wind speeds, the products (KH_{1ij}^*) and ($K^2H_{3ij}^*$) are very nearly frequency independent and are approximated well with quasi-steady lift in this flat, frequency independent range.

The step size in all simulations is 0.04 seconds. Bridge motions are simulated for a duration of 10 minutes (15,000 total steps in the simulation)

APPENDIX 4
IDENTIFICATION PROCEDURE FOR FLUTTER DERIVATIVES FROM SECTION MODEL TESTS

A linear description of the motion of this section model, for small motions, is

$$m(d^2h / dt^2) + c_h(dh / dt) + k_h h = LI \qquad (4.1)$$

$$I(d^2\alpha / dt^2) + c_\alpha(d\alpha / dt) + k_\alpha \alpha = MI \qquad (4.2)$$

where

m	mass of section model;
I	rotational inertia of section model;
c_h	damping coefficient for vertical motion
c_α	damping coefficient for torsional motion
k_h	vertical stiffness;
k_α	torsional stiffness; and
l	model length.

L and M, and positive coordinate and action directions are presented in Appendix 3.

It is assumed here that the bridge deck is symmetrical about its centerline, so there are no mechanical coupling terms. The linear description of the motion is valid because motions are constrained to be very small. Any motion that becomes large is of academic interest only, and is to be avoided at all costs by the bridge designer. If a large motion is expected over the life span of the bridge, the bridge deck geometry, structure, or energy dissipation capability is changed until that motion is again expected to be small. The linear description of small bridge structure motions is well established.

In this form, all of the aeroelastic flutter coefficients are dimensionless. For the description of the identification procedure here, consider the simplified description

$$(d^2h / dt^2) + 2\omega_h\zeta_h(dh / dt) + \omega_h{}^2 h = H_1(dh / dt) + H_2(d\alpha / dt) + H_3\alpha + H_4 h \qquad (4.3)$$

$$(d^2\alpha / dt^2) + 2\omega_\alpha\zeta_\alpha(d\alpha / dt) + \omega_\alpha{}^2\alpha = A_1(dh / dt) + A_2(d\alpha / dt) + A_3\alpha + A_h h \qquad (4.4)$$

where

$$\omega_h{}^2 = k_h \; m$$

$$\omega_\alpha^2 = k_\alpha \quad I$$

$$\zeta_h = c_h \quad 2\omega_h m$$

$$\zeta_\alpha = c_\alpha \quad 2\omega_\alpha I$$

and Hi and Ai are related to their respective Hi* and Ai* in an obvious manner. Again the Hi and Ai are not constants, but are functions of the wind speed U, or the reduced velocity U/nB, or a form of its inverse (the reduced frequency) K = ωB/U.

Let Equations 4.3 and 4.4 be rearranged one more time for convenience, to the following form:

$$(d^2h / dt^2) + (2\omega_h\zeta_h - H_1)(dh / dt) + (\omega_h^2 - H_4)h = H_2(d\alpha / dt) + H_3\alpha \qquad (4.5)$$

$$(d^2\alpha / dt^2) + (2\omega_\alpha\zeta_\alpha - A_2)(d\alpha / dt) + (\omega_\alpha^2 - A_3)\alpha = A_1(dh / dt) + A_4h \qquad (4.6)$$

Consider first, the single Equation 4.5. This is simply the equation of motion of a single-degree-of-freedom oscillator with dynamic response characteristics ω and ζ where

$$\omega^2 = \omega_h^2 - H_4 \qquad (4.7)$$

and

$$2\zeta\omega = 2\zeta_h\omega_h - H_1 \qquad (4.8)$$

subject to the forcing function $F(t) = H_2(d\alpha / dt) + H_3\alpha$

The frequency ω typically will be close to the circular frequency for vertical motion, ω_h. The general solution to this equation (4.5) for an interval of time from t_1 to t_2, can be described as a linear combination of four solutions:

$$h(t) = Y_1y_1(t) + Y_2y_2(t) + Y_3y_3(t) + Y_4y_4(t) \qquad (4.9)$$

where

$y_1(t)$ the response of the oscillator to a unit displacement at t_1;

$y_2(t)$ the response of the oscillator to a unit velocity at t_1;

$y_3(t)$ the response of the oscillator to the "forcing function", (dα / dt), with zero initial conditions at t_1; and

$y_4(t)$ the response of the oscillator to the "forcing function", α(t), with zero initial conditions at t_1; and

The coefficients Y_1, Y_2, Y_3, and Y_4 are assumed, in this linear representation of the motion, to be constants for a given ω, ζ, and reduced velocity U/nB for the particular test.

The four solutions are transient solutions. The solutions $y_1(t)$ and $y_2(t)$ are obviously exponentially varying (not necessarily decaying) harmonic functions with circular frequency, ω, and viscous damping coefficient, ζ (which is not necessarily positive). Since the torsional motions of the section model, $\alpha(t)$ and $\alpha(t)$, are also likely to be exponentially varying harmonic motions, the responses $y_3(t)$ and $y_4(t)$ are likely to be as well. These responses, $y_3(t)$ and $y_4(t)$, however will have a frequency equal to the circular frequency of the measured torsional motion, which in turn, typically is very close to the still-air torsional frequency, ω_α.

The objective for Equation 4.5 is again to identify, from recorded section model motions h(t) and $\alpha(t)$, and from the wind-off dynamic response characteristics ω_h, ω_α, ζ_h, and ζ_α, the four flutter coefficients H_1, H_2, H_3, and H_4. If ω_h and ζ_h are known (the observed dynamic response characteristics for the vertical motion with wind speed U), then H_1 and H_4 can be determined from Equations 4.7 and 4.8. If the observed response is decomposed in the form of Equation 4.9, then it follows that $H_2 = Y_3$ and $H_3 = Y_4$. A combined exhaustive search procedure (educated trial and error approach) and a linear-least-squares fitting procedure in the time domain is used to identify ω, ζ, Y_3, and Y_4.

In order for the response to be decomposed into the four transient responses as defined by Equation 4.9, the section model test set-up must be designed specifically to make that decomposition possible. All four transient responses, $y_1(t)$, $y_2(t)$, $y_3(t)$, and $y_4(t)$ are exponentially varying harmonic functions. If the vertical motion frequency and the torsional motion frequency are similar, there is no way that the response can be decomposed *uniquely* as shown in Equation 4.9. Whether or not the frequencies are separated, in reality, for the full-scale bridge, they must be separated in the section model test if this procedure is to be used. Since the objective from the section model test is to determine the flutter coefficients (not simulate the actual bridge behavior), the two section model frequencies can be separated as much as possible, by any amount that is convenient, in order to maximize the accuracy of the data to be collected. Once the flutter coefficients have been identified, they then can be used in an analytical model of the full bridge, including all modes of vibration, as outlined in Ref 1 to predict the critical flutter velocities, should they exist.

The precise identification procedure (for coefficients H_1, H_2, H_3, and H_4 from Equation 4.5) follows directly:

Define one more response

$$X(t) = Y_1y_1(t) + Y_2y_2(t) + Y_3y_3(t) + Y_4y_4(t) \qquad (4.10)$$

where the Y's and the y(t)'s are defined as before, for $t_1<t<t_2$. If the Y's, ω, and ζ will be found such that the squared error E

$$E = \int_{t_1}^{t_2} (X(t) - h(t))^2 dt \qquad (4.11)$$

is least.

First, for a given wind speed U, the model is perturbed such that significant, but still small, vertical and torsional motions are produced. A sample of the transient motions (either decaying motions or diverging motions) is recorded, i.e., h(t) and α(t) for $t_1<t_2$. It is assumed that the wind-off dynamic response characteristics have previously been recorded.

Second, values of ω and ζ are assumed. For this set of values, a linear-least-squares fitting procedure is used to determine the optimal values of Y_1, Y_2, Y_3, and Y_4, and the squared error E is computed using Equation 4.11. A modified version of a steepest descent procedure is used, with respect to the variables ω and ζ (and at each step the best-fit values of Y_1, Y_2, Y_3, and Y_4 are recalculated). In this manner an optimal set of ω, ζ, Y_1, Y_2, Y_3, and Y_4, are found from which the H_1, H_2, H_3, H_4, and in turn, the H_1^*, H_2^*, H_3^*, and H_4^* are found. It is assumed that these best-fit values of the flutter coefficients are in fact the best estimates of those true values for the section model.

The exact procedure is repeated using Equation 4.6 to determine the torsional flutter coefficients A_1^*, A_2^*, A_3^* and A_4^*.

There is no way to prove that this procedure will converge to the proper values of the flutter coefficients, but years of use seems to indicate that it will. Again, there is the possibility that a set of flutter coefficients is found that is locally optimal, but not globally optimal. The likelihood of that occurring is greatly reduced if small steps are made in incrementing the wind speed from one speed to another, and if the previous best-fit values of ω and ζ are used as initial estimates for the next wind speed (starting with wind-off values for the first step).

This identification procedure relies heavily upon the assumption that the mechanical vibrations of the model, and the unsteady aerodynamic loads are linear functions of the model motion. Shown on Figure 4.1, 4.2, and 4.3 are sets of two curves of A_2^* and H_1^* that were obtained for two different bridge sections. One A_2^* curve in a set was obtained from observed torsional motions with the vertical motion suppressed. The second A_2^* curve in the set was obtained using the procedure described in this paper from torsional motions that were superimposed upon vertical motions. Similarly, one H_1^* curve in a set was obtained from observed vertical motions with torsional motion suppressed. The second H_1^* curve in the set was obtained using the procedure described in this paper from vertical motions that were superimposed upon torsional motions. The good agreement between the two curves in each set verifies that validity of the assumption of linearity in the aerodynamic loads.

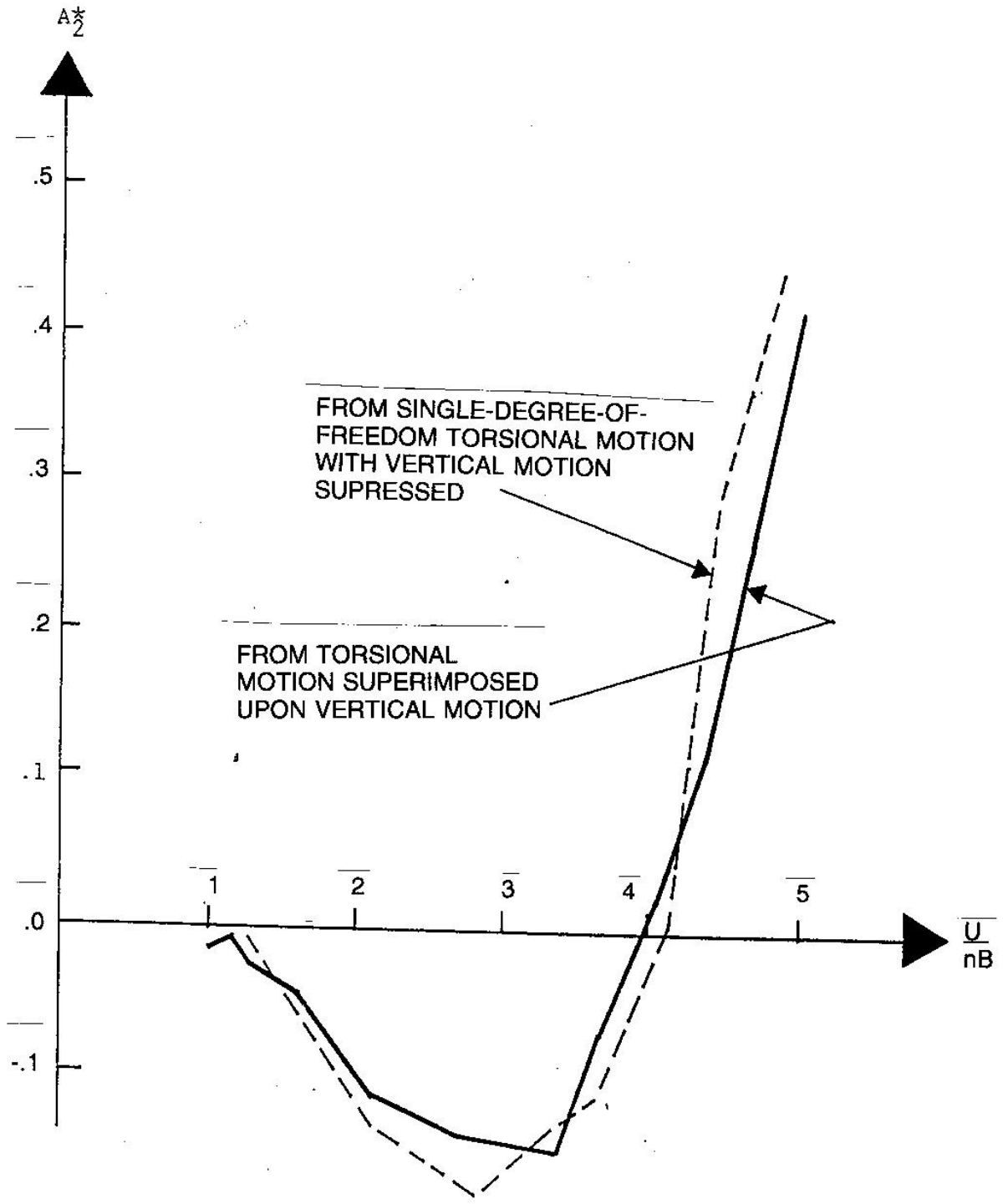
A*z
.5
.4
.3
.2
.1
.0
-.1
FROM SINGLE-DEGREE-OF-FREEDOM TORSIONAL MOTION WITH VERTICAL MOTION SUPRESSED
FROM TORSIONAL MOTION SUPERIMPOSED UPON VERTICAL MOTION
1
2
3
4
5
U/nB

FIGURE 4.01

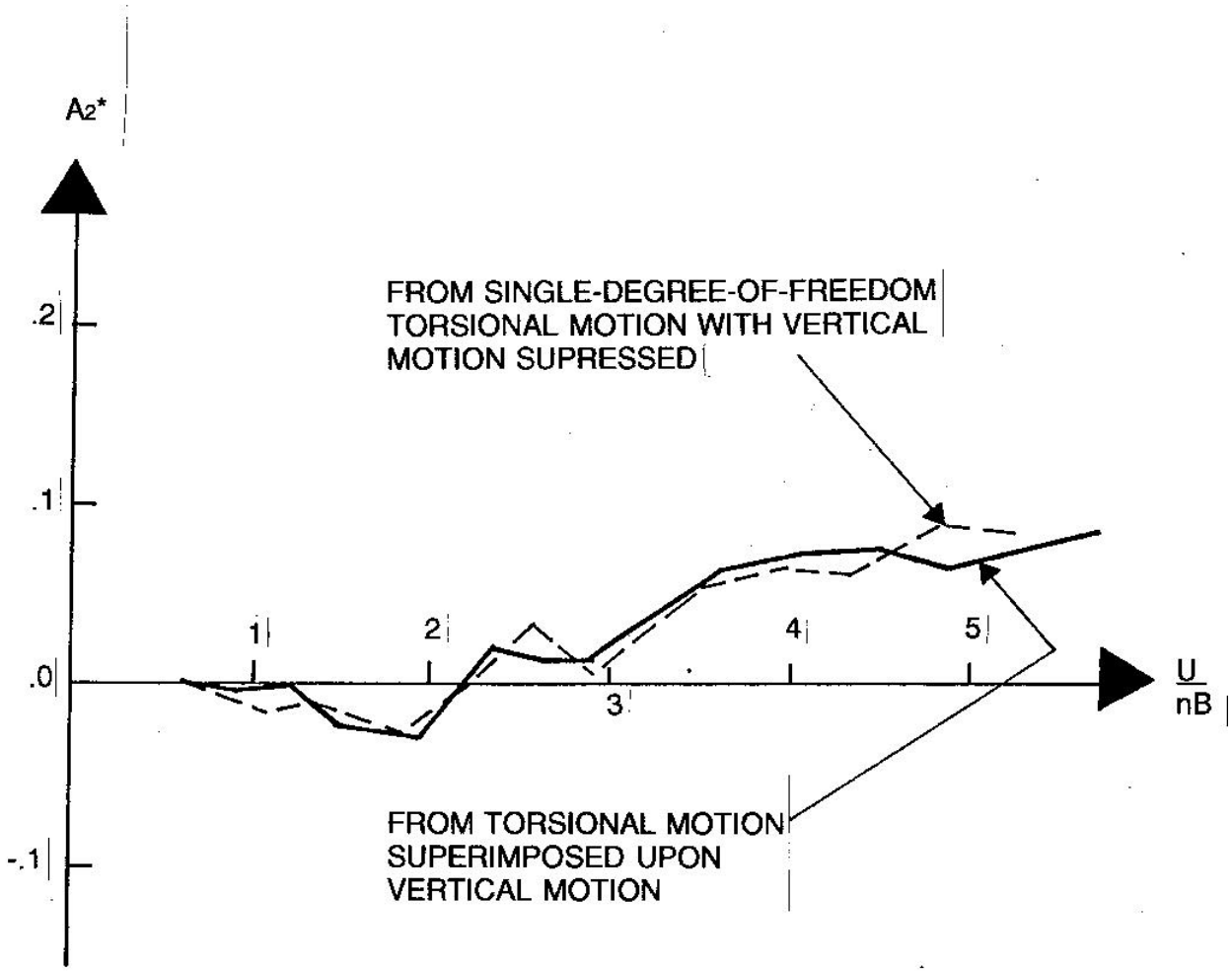
A2*
.2
.1
.0
-.1
1
2
3
4
5
U
nB
FROM SINGLE-DEGREE-OF-FREEDOM
TORSIONAL MOTION WITH VERTICAL
MOTION SUPRESSED
FROM TORSIONAL MOTION
SUPERIMPOSED UPON
VERTICAL MOTION

FIGURE 4.02

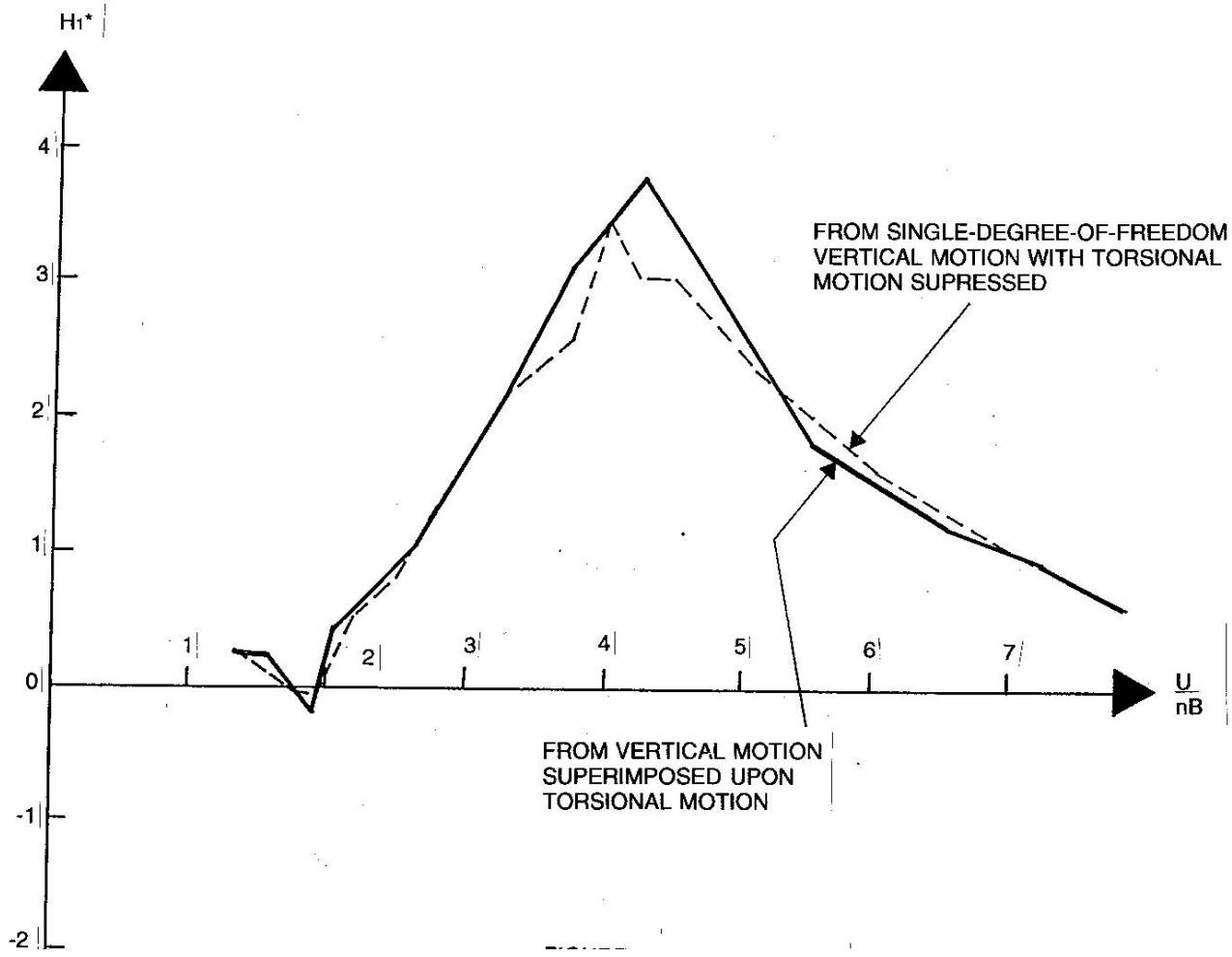
H1*
4
3
2
1
0
-1
-2
1
2
3
4
5
6
7
U
nB
FROM SINGLE-DEGREE-OF-FREEDOM
VERTICAL MOTION WITH TORSIONAL
MOTION SUPRESSED
FROM VERTICAL MOTION
SUPERIMPOSED UPON
TORSIONAL MOTION

FIGURE 4.03